Current Biology, Volume *34*

Supplemental Information

Transcranial magnetic stimulation effects support an oscillatory model of ERP genesis

Jelena Trajkovic, Francesco Di Gregorio, Gregor Thut, and Vincenzo Romei

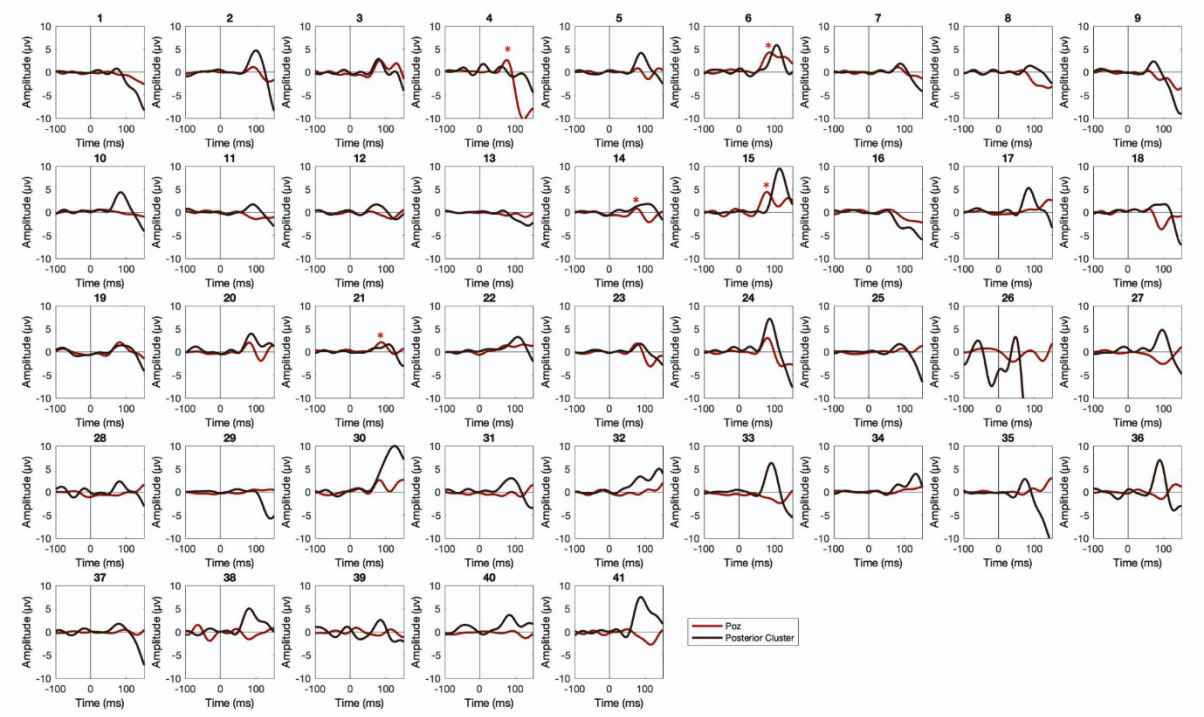

Figure S1. C1 and P1 in Single Subject ERPs. Related to Figure1. Single-subject C100 and P100 plots. For each subject of the Experiment 1 the averaged ERPs at electrode PoZ (red line) and in the posterior cluster (O2, Po4, Po8, black line) are reported. * identifies those subjects with a distinguished C1 and P1 components. ms = milliseconds; μv = microvolt.

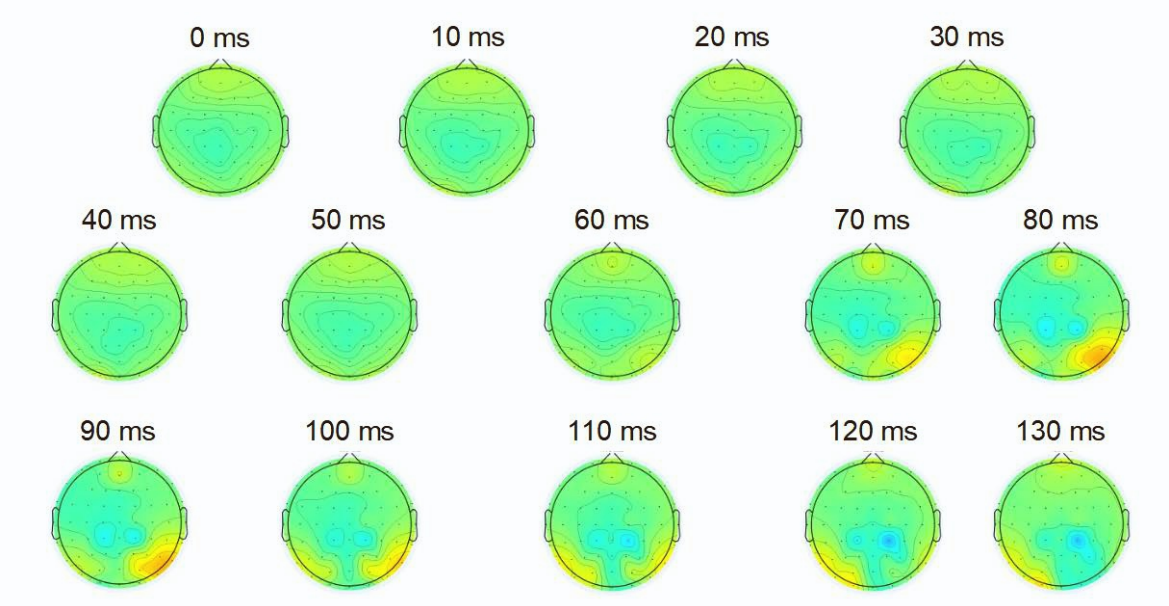

Figure S2. **Topographies from 0 to 130 ms. Related to Figure 1.** 10 milliseconds moving Topographies between Stimulus presentation and 130 ms after. The topographies show a first positive peak in the hemisphere contralateral to the stimulus location (right hemisphere) around 70-80 ms after stimulus, corresponding to the P1 time window.

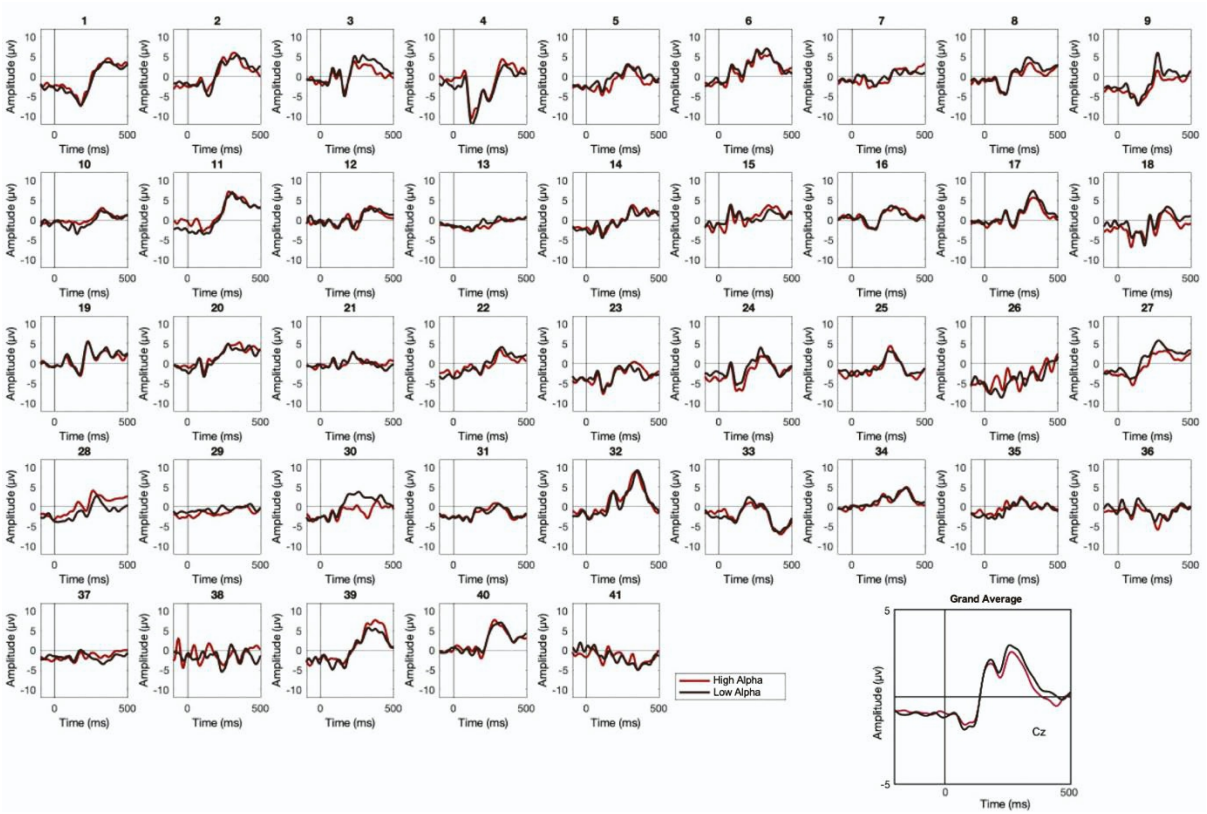

Figure S3. P300 in high vs. low Alpha Amplitude Trials: Single-subject P300 plots. Related to Figure 1. For each subject of the Experiment 1, trials were first sorted in 3 bins (high-medium and low prestimulus alpha-amplitude) then the averaged ERPs at electrode Cz are reported for trials with high prestimulus alpha-amplitude (red line) and low prestimulus alpha-amplitude (black line). Grandaverage at electrode Cz is also reported in the lower panel. ms=milliseconds; μv = microvolt.

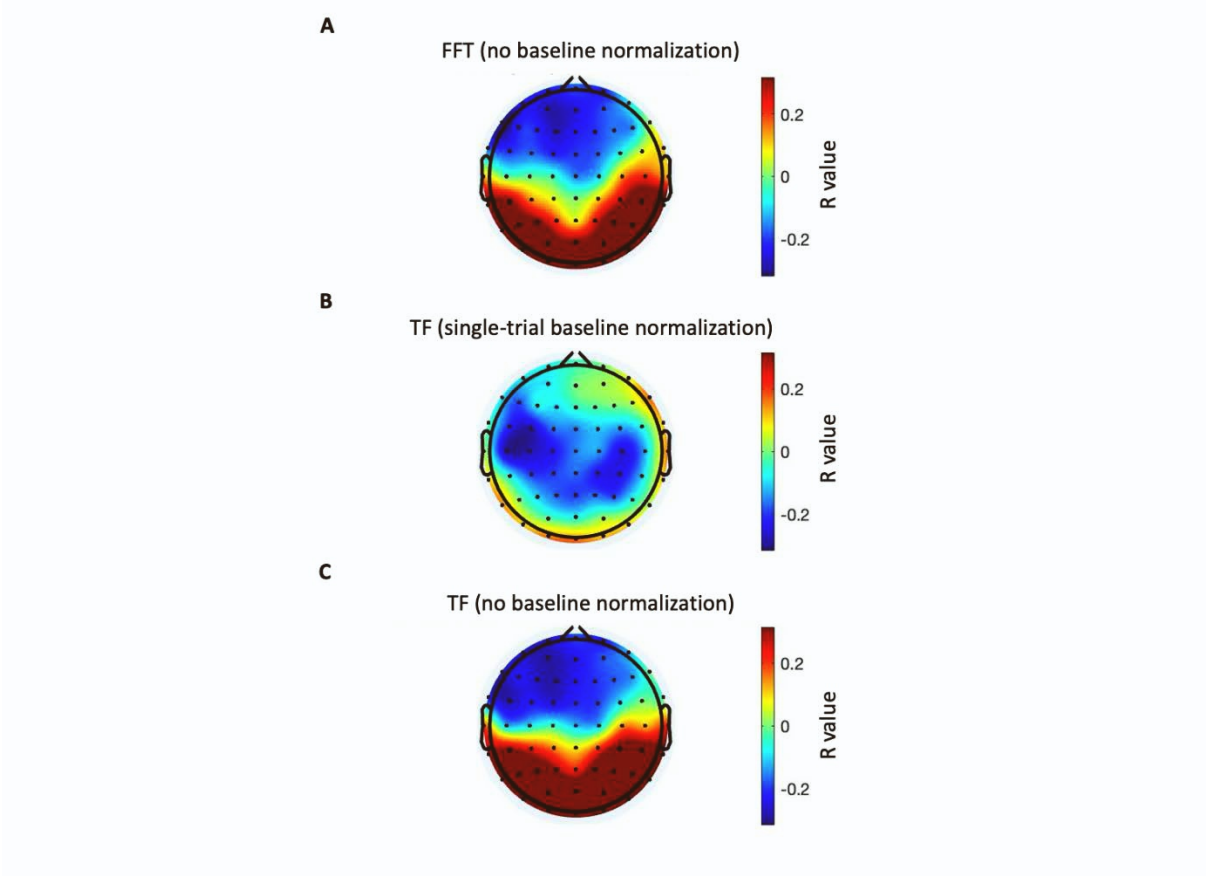

Figure S4. **Correlation Topographies between Alpha and P300 amplitude. Related to Figure 2.** Whole brain correlational analyses for Experiment 1. The topographies reflect the Pearson R correlational coefficients between pre-stimulus alpha-amplitude and P300 amplitude over each scalp electrode. Specifically, we calculated the correlations between pre-stimulus alpha-amplitude over parieto-occipital electrodes (i.e., O2, Po4 and Po8) and P300 amplitude over each electrode, using different approaches. **A**. Scalp distribution of the correlation coefficients between P300 amplitude and alpha-amplitude calculated by FFT analyses with no baseline normalization. The topography shows the effect of posterior alpha-amplitude on the P300 amplitude, with positive links between alpha and P300 across occipital and occipito-parietal electrodes which can be explained via baseline shift. **B**. Scalp distribution of the correlation coefficients between P300 amplitude and alpha-amplitude calculated by TF analyses with single-trial baseline normalization. This baseline normalization approach puts emphasis on a short-term variability of alpha-amplitude right before the visual stimulus, while reducing long-term, sustained variability. The topography shows the effect of posterior alpha-amplitude on the P300 amplitude, with negative links between alpha and P300 across a broad central electrode cluster which can be explained via the functional inhibition mechanism. Notably, the Scalp distribution of the correlations closely resembles the topography of the P300 in the Experiment 1 (see Figure 1B) **C**. Scalp distribution of the correlation coefficients between P300 amplitude and alpha-amplitude calculated by TF analyses with no baseline normalization. The topography shows the effect of posterior alpha-amplitude on the P300 amplitude, with positive links between alpha

and P300 across occipital and occipito-parietal electrodes resembling Figure A. These results confirm that multiple coexisting mechanisms bind the alpha-amplitude and P300, whereas different analysis approaches make one or the other mechanism more visible (see test below for a detailed account). FFT , Fast Fourier Transformation; TF, Time Frequency. This figure clarifies the discrepancy in direction of the prestimulus alpha- vs. P300-amplitude link - in light of the flip of directionality with slightly different analyses approaches and electrode selection (see main text of manuscript). To reveal the source of the discrepancy, we conducted follow-up analyses on data of Experiment 1. More specifically, we conducted a whole-brain correlational analysis using both TF and FFT. Specifically, we correlated pre-stimulus alpha- over parieto-occipital and occipital sensors with P300-amplitude over the whole scalp, using TF and FFT (Figure S4A and S4B). Comparing the two approaches regarding the effect of posterior alpha-amplitude on the P300 amplitude, we notice qualitatively different topographies, with positive links between alpha and P300 across posterior clusters for the FFT analysis (can be explained via baseline shift), and negative clusters for the TF analysis instead (in line with a functional inhibition account). Please note that the topography of the FFT correlational map (Figure S4A) shows occipito-parietal positivity (occipito-parietal alpha correlates positively with late post-stimulus ERP/P300 amplitude over the same sensors), whereas the TF correlational map (Figure S4B) shows a centro-parietal negativity which mirrors in topography the P300 that we observed to be correlated with the perceptual outcome (cf manuscript Figure 1B: note the typical centro-parietal P300 topography). Hence, for this latter map, it is posterior alpha-activity that negatively correlates with a perceptually relevant centro-parietal P300 activity. It is worth noting that one would expect baseline shift mechanism not only to be expressed by positive alpha-ERP correlations but these correlations also to be spatially restricted to the occipito-parietal origin of the alpha activity, and to vanish for more central sites (as observed in Figure S4A). This is because as per the baseline shift model, the late evoked responses should mirror the ERD of pre-stimulus alpha-activity in timing and topography. On the other hand, the finding of occipito-parietal alpha to be negatively correlated with more remote, central P300 activity (as revealed in Figure S4B) is in line with a functional inhibition account. Because of its match to the perceptually relevant P300-component, we argue that it is this latter relationship that is functionally interpretable in the context of our visual task/ probes. Where do these differences in correlation topography originate from, and are they physiologically meaningful? One crucial aspect that differs between the above two analyses approaches is the use of an additional single-trial baseline normalization for the TF analysis, commonly used to tackle the problems of 1/f power scaling and subject-specific and electrode-specific idiosyncratic characteristics [S1], not applied for FFT. Moreover, this additional baseline correction puts emphasis on short-term (within-trial) variability of alpha-changes right before the visual stimulus, because normalizing longer-term, sustained variability in alpha. Specifically, our choice of baseline is forcing the variability to be captured in a 1000ms pre-stimulus window. Importantly, it is within this 1000ms window where many previous studies have found short-term alpha-fluctuations to covary with upcoming perception [S2–S6]. To test whether it is indeed the additional baseline normalization during TF that may have caused the difference in correlation topography (not the use of TF vs. FFT), we repeated the TF analysis but without the additional baseline normalization (Figure S4C). This revealed qualitatively comparable results to the FFT analysis (Figures S4C vs S4A), thus confirming the additional baseline normalization to be the source

of the differences. Based on these observations, we conclude that there are likely two alpha-contributors to P300 variability: one that is based on alpha-changes that are sustained over many trials (and is e.g., underpinned by baseline shift), the contribution of which is minimized by baseline normalization within trials. And another that is more short-term, and hence may be uncovered when long-term changes are parceled out. In brief, these new results indicate the presence of two alpha-contributors to the P300-amplitude, that are differentially emphasized depending on chosen analysis approaches. Only one of them is functionally interpretable in our task context.

Supplemental References

S1. Cohen, M. (2014). Analyzing Neural Time Series Data: Theory and Practice (MIT Press).

S2. Romei, V., Brodbeck, V., Michel, C., Amedi, A., Pascual-Leone, A., and Thut, G. (2008). Spontaneous fluctuations in posterior alpha-band EEG activity reflect variability in excitability of human visual areas. Cereb Cortex 18, 2010–2018. 10.1093/cercor/bhm229.

S3. Samaha, J., Iemi, L., and Postle, B.R. (2017). Prestimulus alpha-band power biases visual discrimination confidence, but not accuracy. Conscious Cogn 54, 47–55. 10.1016/j.concog.2017.02.005.

S4. Samaha, J., Iemi, L., Haegens, S., and Busch, N.A. (2020). Spontaneous Brain Oscillations and Perceptual Decision-Making. Trends Cogn Sci 24, 639–653. 10.1016/j.tics.2020.05.004.

S5. Benwell, C.S.Y., Tagliabue, C.F., Veniero, D., Cecere, R., Savazzi, S., and Thut, G. (2017). Prestimulus EEG Power Predicts Conscious Awareness But Not Objective Visual Performance. eNeuro 4, ENEURO.0182-17.2017. 10.1523/ENEURO.0182-17.2017.

S6. Iemi, L., Chaumon, M., Crouzet, S.M., and Busch, N.A. (2017). Spontaneous Neural Oscillations Bias Perception by Modulating Baseline Excitability. J Neurosci 37, 807–819. 10.1523/JNEUROSCI.1432-16.2016.